Advances in Nano Research, *Vol. 7 No. 2 (2019) 125-134*
DOI: https://doi.org/10.12989/anr.2019.7.2.125

The relationship between precursor concentration and antibacterial activity of biosynthesized Ag nanoparticles

Matej Baláž [*1], Ľudmila Balážová [2], Mária Kováčová [1,2], Nina Daneu [3], Aneta Salayová [4], Zdenka Bedlovičová [4] and Ľudmila Tkáčiková [5]

[1] *Department of Mechanochemistry, Institute of Geotechnics, Slovak Academy of Sciences, Watsonova 45, 04001 Košice, Slovakia*
[2] *Department of Pharmacognosy and Botany, University of Veterinary Medicine and Pharmacy, Komenského 73, 04181 Košice, Slovakia*
[3] *Advanced Materials Department, Jožef Stefan Institute, Jamova 39, 1000 Ljubljana, Slovenia*
[4] *Department of Chemistry, Biochemistry and Biophysics, Institute of Pharmaceutical Chemistry, University of Veterinary Medicine and Pharmacy, Komenského 73, 04181 Košice, Slovakia*
[5] *Department of Microbiology and Immunology, University of Veterinary Medicine and Pharmacy, Komenského 73, 04181 Košice, Slovakia*

(*Received October 30, 2018, Revised March 2, 2019, Accepted April 5, 2019*)

Abstract. The *Origanum vulgare* L.-mediated synthesis of Ag nanoparticles was successfully realized within the present study. Various concentrations of the $AgNO_3$ used as a silver precursor (1, 2.5, 5, 10 and 100 mM) were used. Very rapid formation of Ag nanoparticles was observed, as only minutes were necessary for the completion of the reaction. With the increasing concentration, red shift of the surface plasmon resonance peak was observed in the Vis spectra. According to photon cross-correlation spectroscopy results, the finest grain size distribution was obtained for the 2.5 mM sample. The transmission electron microscopy analysis of this sample has shown bimodal size distribution with larger crystallites with 100 nm size and smaller around 10 nm. The antibacterial activity was also the best for this sample so the positive correlation between good grain size distribution and antibacterial activity was found. The in-depth discussion of antibacterial activity with related works from the materials science point of view is provided, namely emphasizing the role of effective nanoparticles distribution within the plant extract or matrix. The antibacterial activity seems to be governed by both content of Ag nanoparticles and their effective distribution. This work contributes to still expanding environmentally acceptable field of green synthesis of silver nanoparticles.

Keywords: silver nanoparticles; green synthesis; antibacterial activity; *Origanum*

1. Introduction

Silver nanoparticles (Ag NPs) have an inevitable place among the mostly researched topics these days (McGillicuddy *et al*. 2017, Pandiarajan and Krishnan 2017, Syafiuddin *et al*. 2017, Kang *et al*. 2019), mostly due to their well-known antibacterial activity against rich plethora of bacteria (Rai *et al*. 2009, Franci *et al*. 2015, Deshmukh *et al*. 2019, Liao *et al*. 2019, Mabey *et al*. 2019). Ag NPs also prevent bacterial biofilm formation (Roe *et al*. 2008, Nookala *et al*. 2015), exhibit anticancer activity (Malik and Mukherjee 2018) or are applied as photocatalysts (Gellé and Moores 2019). They can be prepared by a wide variety of methods (Abou El-Nour *et al*. 2010, Iravani *et al*. 2014, Beyene *et al*. 2017). However, some of these are harmful to the environment and therefore, the green synthesis using natural products as reducing agents is being more and more applied these days (Sharma *et al*. 2009, Sur 2014, Rajan *et al*. 2015, Ahmed *et al*. 2016, de Souza *et al*. 2019, Fahimirad *et al*. 2019, Roy *et al*. 2019). Myriad of plant extracts has been used for the synthesis of Ag NPs, as can be traced down in recent literature (Upadhyay and Verma 2015, Ahmed *et al*. 2016). Among those plants, *Origanum vulgare* L. is of high interest, because of high content of potential reducing substances, health-beneficial properties and easy availability (Liang *et al*. 2012, Abbasi *et al*. 2015). The synthesis of nanoparticles using this plant was already reported by classical green approach (Sankar *et al*. 2013), followed by applying wet stirred media milling in polyvinyl pyrrolidone solution for stabilization (Baláž *et al*. 2017a) or completely solid-state approach (Baláž *et al*. 2017b Very recently, a paper reporting on the antibacterial activity and properties of the Ag nanoparticles produced by using different amounts of the *Origanum vulgare* L. plant extract was published (Shaik *et al*. 2018).

Among many parameters influencing the synthesis of Ag NPs like temperature (Lee *et al*. 2014) or pH (Velgosova *et al*. 2016), also the concentration of the precursor can have a significant influence on the final properties of the prepared nanoparticles. This can result in different shape, size or some other characteristics. The reaction speed is also influenced. The parameter belongs among the key ones, so it is often discussed in various review papers as a tool for controllable synthesis of Ag NPs. The particular results on this topic can be found in research papers (e.g., in (Khan *et al*. 2014, Roy *et al*. 2014, Ibrahim 2015, Maria *et al*. 2015, Rao and Tang 2017)). However, as pointed out in (Shaik *et al*. 2018), a comparative investigation of the ability of plant extracts of the same plant from different origins is highly

*Corresponding author, Ph.D.,
E-mail: balazm@saske.sk

Copyright © 2019 Techno-Press, Ltd.

ISSN: 2287-237X (Print), 2287-2388 (Online)

desirable, herein we provide a report on the *Origanum vulgare* L. of Slovak origin. Moreover, it offers plenty of room for discussion with the results of the mentioned study and different perspective, as in our case, the amount of $AgNO_3$ in the system was changed, whereas in the other publication (Shaik *et al*. 2018), it was fixed and different amounts of extract were added to the solution. Thus, both approaches lead to the change in plant-to-$AgNO_3$ ratio, which can be compared.

In the present work, in addition to the successful green synthesis of Ag NPs using *Origanum vulgare* L. plant extract, different concentrations of the $AgNO_3$ precursor were used and the antibacterial activity was positively correlated with the results obtained with the photon cross-correlation spectroscopy measurements, on the contrary to other papers, in which mostly only UV-Vis spectra were used for evaluation of the precursor concentration effect. *Origanum vulgare* L. extract was selected because of the high abundance of the plant and because the extracted water-soluble compounds possess very strong reducing ability. The in-depth discussion regarding the effect of precursor concentration on the antibacterial activity is also provided, which is also scarce in most papers reporting the green synthesis of Ag NPs.

2. Experimental

2.1 Materials

Silver nitrate ($AgNO_3$, 99.9%, Mikrochem, Slovakia) was used without further purification. *Origanum vulgare L*. plants were collected in summer from the meadow in University of Veterinary Medicine and Pharmacy campus in Košice, Slovakia.

2.2 Preparation of Origanum vulgare L. extract

The procedure from ref. (Sankar *et al*. 2013) was repeated. Namely, leaves of the *Origanum vulgare* L. plants were dried up to constant weight in dark at room temperature. The dried leaves were powdered to fine particles by kitchen mixer (type HR2061, Philips, Netherlands). *Origanum vulgare* L. extract was prepared by suspending 5 g of the dry powder into 50 mL of distilled water. The mixture was heated at 60℃ for 10 min and after cooling down, the solid residues were removed and the filtrate was used for the synthesis of nanoparticles.

2.3 Plant-mediated synthesis of Ag NPs

Silver nitrate water solutions with the concentrations 1, 2.5, 5, 10 and 100 mM were prepared just before application under dark conditions to prevent decomposition. During continuous stirring by magnetic stirrer, 90 mL of $AgNO_3$ solution was heated up to 80℃ and 10 mL of *Origanum vulgare L*. water extract was slowly added and incubated in the temperature range 75-85℃ using a water bath. The formation of Ag NPs was observed by transformation from the light brownish yellow to the dark brownish red color. Thus, the procedure reported in Sankar *et al*. (2013) was repeated also for the Ag NPs synthesis.

2.4 Antibacterial activity

The antibacterial properties of the samples were evaluated by the agar well diffusion method by slight modification of the process reported in Rojas *et al*. (2006). The tested bacteria (*Staphylococcus aureus* CCM 4223, *Bacillus cereus* CCM2010, *Listeria monocytogenes* CCM 4699, *Escherichia coli* CCM 3988, *Salmonella enterica ser. Typhimurium* CCM 7205, and *Pseudomonas aeruginosa* CCM 3989) were obtained from the Czech collection of microorganisms (CCM).

In brief, bacteria were cultured aerobically at 37 ℃ in nutrient broth (Oxoid, United Kingdom) with agitation or on standard plate count agar (Oxoid, United Kingdom). Frozen stock cultures were maintained at -20℃. Before the experimental use, cultures were transferred to the liquid media and incubated for 24 h. Cultures were then subcultured in liquid media, incubated for 24 h, and used as the source of inoculum for each experiment.

Agar media was cooled to 42℃ after autoclaving, inoculated with liquid overnight bacterial culture to a cell density of 5×10^5 cfu/mL and 20 mL of this inoculated agar was pipetted into a 90-mm diameter Petri dish. Once the agar was solidified, five millimeters diameter wells were punched in the agar and filled with 50 μL of the prepared nanosuspensions. Distilled water was used as negative control and gentamicin sulfate (Sigma-Aldrich, USA) with the concentration 10 mM as a positive control. The plates were incubated for 24 h at 37℃. After the incubation, the plates were photographed and the inhibition zones were measured by the ImageJ software. The values used for the calculation were mean values of 3 replicate tests.

The antibacterial activity was calculated according to the study (Rojas *et al*. 2006) by applying the formula

$$\%RIZD = \left[\frac{\text{IZD sample} - \text{IZD negative control}}{\text{IZD positive control}}\right] \times 100 \quad (1)$$

where RIZD is the relative inhibition zone diameter (%) and IZD is the inhibition zone diameter (mm).

2.5 Characterization methods

The progress of Ag NPs formation was monitored by recording Vis spectra using the Cary 60 UV-Vis spectrophotometer (Agilent Technology, Malaysia).

Particle size distribution of the nanosuspensions was measured by a photon cross-correlation spectroscopy using a Nanophox particle size analyzer (Sympatec, Germany). A portion of each nanosuspension was diluted with distilled water to achieve a suitable concentration for the measurement. This analysis was performed using a dispersant with the refractive index of 1.33. The measurements were repeated 3 times for each sample.

The sample with 2.5 mM of silver nitrate was additionally inspected by transmission electron microscopy (TEM). A droplet of the nanosuspension was applied on

Table 1 Comparison of selected experimental conditions of studies dealing with *Origanum vulgare* L.-mediated synthesis of Ag nanoparticles

Sample notation in the paper	OV : water ratio when preparing extract	V extract (mL)	V $AgNO_3$ solution (mL)	c $AgNO_3$ solution (mM)	m $AgNO_3$ in reaction mixture (mg)	m OV in reaction mixture (mg)	$AgNO_3$:OV ratio weight ratio	Ref.
Ag NPs	0.1 (5 g OV to 50 mL H_2O)	10	90	1	15	1000	0.02	(Sankar *et al*. 2013, Baláž *et al*. 2017a) [1]
Ag-ORE	-	-	-	-	1500	1500	1	(Baláž *et al*. 2017a)
OV-Ag-1	0.22 (550 g OV to 2500 mL H_2O)	1	49	10.2	85	220	0.39	(Shaik *et al*. 2018)
OV-Ag-2		2.5	47.5	10.5	85	550	0.15	
OV-Ag-3		5	45	11.1	85	1100	0.08	
OV-Ag-4		7.5	42.5	11.8	85	1650	0.05	
1 mM	0.1 (5 g OV to 50 mL H_2O)	10	90	1	15	1000	0.02	This work
2.5 mM		10	90	2.5	38	1000	0.04	
5 mM		10	90	5	77	1000	0.08	
10 mM		10	90	10	153	1000	0.15	
100 mM		10	90	100	1529	1000	1.53	

[1] in ref. Baláž *et al*. (2017a), flowers, stems and leaves were used for the extract preparation, whereas in other cases, only leaves were used

carbon-coated nickel grid. The dried sample was additionally coated with a thin layer of carbon to prevent charging under the electron beam. TEM analysis was performed using a 200 kV microscope JEM 2100 (JEOL, Japan) with LaB_6 electron source and equipped with energy dispersive X-ray spectrometer (EDS) for chemical analysis.

3. Results and discussion

3.1 Synthesis procedure

As already outlined in introduction, a very close study to ours was published recently (Shaik *et al*. 2018). Altogether, there were four studies on *Origanum vulgare* L. (OV)-mediated Ag NPs synthesis until now. In Table 1, the comparison of experimental conditions from all these studies is provided, as it will be very important when discussing results further. Mainly the comparison with the study published by Shaik *et al*. (2018) is important. As it can be seen, the extract in the mentioned study was 2.2-times weaker than in ours. The overall volume of the reaction mixture was 50 mL and 100 mL in (Shaik *et al*. 2018) and our study, respectively. The authors of Shaik *et al*. (2018) changed the extract and $AgNO_3$ solution volume from 1 to 7.5 mL and 49 to 42.5 mL, respectively, whereas we have kept the parameters constant (10 mL extract and 90 mL $AgNO_3$ solution). The concentrations of the used $AgNO_3$ solution in Shaik *et al*. (2018) were from 10.2 to 11.8 mM, which is by far higher than in most studies dealing with the green Ag NPs synthesis. In our case, we tried to cover large region starting from 1 mM to 100 mM. The actual content of $AgNO_3$ in the reaction mixture was fixed at 85 mg in Shaik *et al*. (2018), whereas in our case it was changed from 15 mg to more than 1.5 g. By changing the amount of extract, the authors of Shaik *et al*. (2018) were changing the dry herb content in the reaction mixture, whereas in our case, this parameter was fixed. It is clear that by changing the dry herb content, the amount of substances capable of reduction and possible stabilization is changed. From the mass of dry $AgNO_3$ and dry weight of herb, the ratio of dry masses can be calculated, and thus, although with limitations, serving as a potentially comparable parameter. It can be seen that this number was decreasing with OV extract content in Shaik *et al*. (2018), whereas it increased with $AgNO_3$ amount in the present study. The calculated parameters will be used in further discussion.

3.2 Vis spectra

The progress of the synthesis of nanoparticles was measured by means of Vis spectroscopy. The synthesis was very rapid for all concentrations. For 1 mM and 2.5 mM concentrations, the Ag NPs formation was finished after 3 and 7 minutes, respectively. For the higher concentrations (10 mM and 100 mM), in spite of NPs, large grains of size of tens of microns were formed and thus, no surface plasmon resonance (SPR) peak could be observed. This can be explained in relation with the content of plant substances, which are oxidized during the process. In the case of higher precursor concentrations, the amount of reduction agents is too small to produce individual nanoparticles, so great bulk particles are being produced, whereas when there is enough reducing agent, NPs are formed.

In Fig. 1(a), the Vis spectra for all concentrations under study are presented. The spectra for the samples for which the synthesis process was completed are presented. It can be seen that the position of the peaks is red-shifted to the higher wavelengths with increasing concentration.

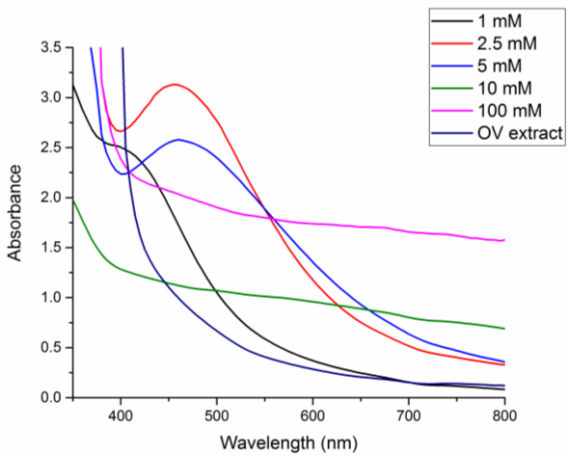

(a) Ag NPs prepared from OV extract and 5 mM $AgNO_3$ at different times

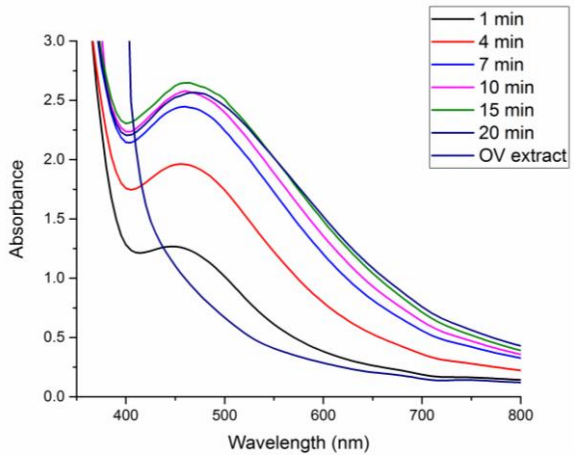

(b) Final samples of Ag NPs prepared from OV extract and various concentrations of $AgNO_3$

Fig. 1 Vis spectra

Concretely, the exact positions of absorbance maxima are 385 nm, 455 nm and 460 nm for 1 mM, 2.5 mM and 5 mM sample. Such red shift was observed also in Shaik *et al.* (2018) with increased amount of OV extract, although the differences were smaller than in our case. The authors explain this by the presence of large amount of reductants and Ostwald ripening. The red shift documents the increase of particle size, in accordance with (Mogensen and Kneipp 2014, Ning *et al.* 2015, Kravets *et al.* 2016).

However, the red shift is also possible if the particles are too small is possible (Peng *et al.* 2010), but we do not have such a small particles in our case. The wavelength of absorbance maximum for Ag NPs synthesized with 1 mM $AgNO_3$ is quite low, pointing to very small nanoparticles in this sample, even smaller than the finest ones reported in Shaik *et al.* (2018). It is much lower than the value obtained in our previous study (445 nm) (Baláž *et al.* 2017a) and in the pilot study (440 nm) (Sankar *et al.* 2013), in which the same concentration was applied. Whereas in former case, it might be caused by the presence of flowers and stems in the starting herb (thus different active compounds), in the latter case the different location of growth could contribute. The wavelengths of absorption maxima obtained for 2.5 mM and 5 mM are in accordance with the majority of studies on Ag NPs preparation. At the concentration 10 mM, the SPR peak was not present, on the contrary to Shaik *et al.* (2018). This is related with the immediate formation of large micro-sized grains probably caused by almost two-times larger $AgNO_3$ content (Table 1). However, the dry weight ratio was the same as in the sample OV-Ag-2 in the similar study and the authors observed nice SPR peak there. As was already discussed, the different growth conditions could completely change the reduction ability of the plant. The slow disappearance of the SPR peak with the increased $AgNO_3$ concentration was observed also in Ibrahim (2015), although in that case, it was observed at lower concentrations and the authors used different natural material for reduction there.

The process of NPs formation could be well observed when using 5 mM $AgNO_3$ (Fig. 1(b)), as it proceeds in a reasonable reaction time and SPR peak is visible. The increase of the absorbance at 450 nm, possibly documenting the formation of spherical NPs (Agnihotri *et al.* 2014) could be observed. The reaction velocity was the highest at the beginning, as can be traced down from the differences among the absorbance in the first minutes of synthesis. This is contrary to study (Shaik *et al.* 2018), where the nucleation started after 90 min. In the present case, the absorbance increased until 10 minutes, and afterwards, it remained the same, thus hinting to the finished reaction. The time of the reaction was shorter than in our previous study, where the combination of leaves, stems and flowers of the same plant were used (Baláž *et al.* 2017a). This is most probably a consequence of the presence of larger amount of substances responsible for the reduction in the leaves. In the first report on OV-mediated Ag NPs synthesis (Sankar *et al.* 2013), the reaction took only 10 min when the concentration 1 mM was used. The reaction velocity was much lower in Shaik *et al.* (2018), where 3 hours were necessary. It might be connected with the different amount of polyphenolic species in *Origanum vulgare* L. grown in different regions. However, as it can be seen from Tab. 1, the authors worked with $AgNO_3$ solutions with concentration higher than 10 mM, which also contributed to the slow process.

3.3 Size distribution and microstructure

In order to investigate grain size distribution of the prepared NPs, the photon cross-correlation spectroscopy (PCCS) measurements were realized for all the studied concentrations. The results are provided in Fig. 2(a). The sample with the finest grains was selected for the TEM analysis (Fig. 2(b)).

The concentration of silver nitrate significantly affects the grain size distribution of the NPs. At lower silver nitrate concentrations (1-5 mM), the average grain size is in the range of 150-300 nm, whereas higher concentrations (10 and 100 mM) lead to the formation of micron-sized agglomerates, also visible to the naked eye. The average

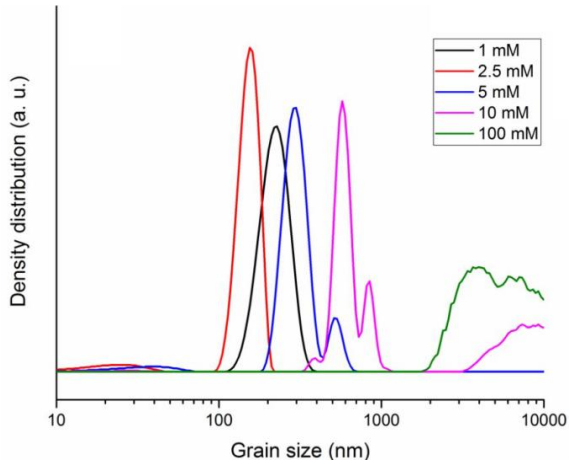

(a) Dependence of grain size distribution of the prepared Ag NPs on the precursor concentration

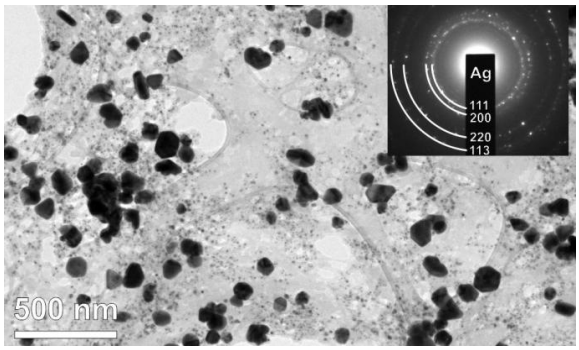

(b) TEM image of the 2.5 mM sample with bimodal particle size distribution. The SAED pattern (inset) confirms that the NPs are crystalline silver (Ag)

Fig. 2 Size distribution and microstructure

hydrodynamic particle diameter, x_{50} was 231, 151, 296, 1224 and 4819 nm for the concentrations 1, 2.5, 5, 10 and 100 mM samples, respectively. The obtained x_{50} value for 1 mM concentration is quite similar to that reported in Baláž *et al*. (2017a) (203 nm), in which the same concentration but the combination of OV flowers, stems and leaves was used. At the same concentration using leaves, 136 nm was registered as an average size by DLS in Sankar *et al*. (2013), so the grains were finer in that case. The PCCS/DLS results for larger concentrations were not reported until now. It is known that the PCCS/DLS method registers the size of grains composed of individual nanoparticles and does not report the actual size of nanocrystals. For that purpose, TEM is much more appropriate method.

The 2.5 mM sample with finest Ag NPs according to the PCCS measurements was additionally inspected by TEM (Fig. 2(b)). The analysis revealed that the sample contains NPs with two distinctly different sizes (bimodal particle size distribution), the larger measure around 100 nm, whereas the smaller ones have average size below 10 nm.

The shape of the particles seems to be polygonal. The crystallinity of the NPs was determined by selected-area electron diffraction (SAED) which confirmed that the particles are silver with the cubic face-centered (copper-type) structure. The ring-pattern indicates completely random orientation of the particles. Both types of Ag NPs are embedded in the organic matrix, where reduction of silver nitrate to silver was initiated due to the presence of active bio-reducing compounds in the water extract of *Origanum vulgare* L. The larger NPs show occasional clustering, which might affect the results of particle size distribution measurements by PCCS, where somewhat larger Ag particle size was detected. The bimodal particle size distribution was observed also in Baláž *et al*. (2017a) for the concentration 1 mM, namely the average size of larger and smaller NPs was 38 and 7 nm, respectively. The presence of AgCl was also evidenced in that case. From the paper (Shaik *et al*. 2018), it is not clear which concentration was analyzed, however, very fine nanoparticles with size ranging from 2 to 25 nm were evidenced. This fineness is actually the strongest point made by the authors, with which they support their long reaction time. Fine particles were also obtained in a completely solid-state approach, in which also bimodal particle size distribution was observed (finer and larger fraction with average size of 3 nm and 34 nm, respectively) (Baláž *et al*. 2017a/b). The comminution surely supports the formation of such small particles. In the pilot study of Ag NPs using OV plant (Sankar *et al*. 2013), TEM was not provided and the particle size was only reported from SEM to be 63-85 nm in that case. From the presented image in that study it seems that it was taken from the agglomerated powder and our opinion is that the actual size of the individual nanoparticles would be much smaller when analyzed by TEM.

3.4 Antibacterial activity

In order to investigate the effect of the precursor concentration and grain size on the antibacterial activity, six different bacterial lines (gram-positive *S. aureus*, *B. cereus*, *L. monocytogenes* and gram-negative *S. enterica ser. Typhimurium*, *E. coli*, *P. aeruginosa*) were tested after the application of the Ag NPs. Each of the bacteria was tested with Ag NPs prepared using different $AgNO_3$ concentration (1, 2.5, 5 and 10 mM) in order to observe the effect on bacterial growth. 100 mM sample was excluded from further consideration because of purely micrometric character of particles. The results for the rest of samples are presented in Fig. 3. The photographs of the Petri dishes containing colonies of gram-positive *S. aureus* and gram-negative *S. typhimurium* after the incubation with the nanoparticles are shown as examples in Fig. 4. The photographs of these two bacterial strains were selected because the prepared Ag NPs showed the best antibacterial performance against them.

The results demonstrated that the prepared silver nanoparticles possess antibacterial activity against all

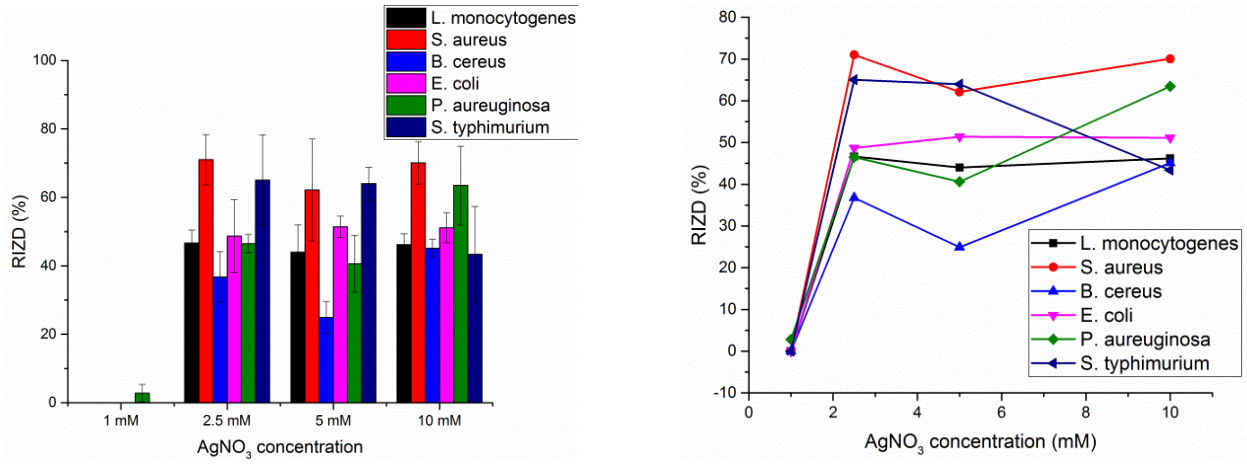

(a) Column graph

(b) Dependence on starting $AgNO_3$ concentration

Fig. 3 Antibacterial activity of silver nanoparticles prepared using different precursor concentrations against various bacterial strains. The antibacterial activity is expressed as %RIZD- the percentage of relative inhibition zone diameter

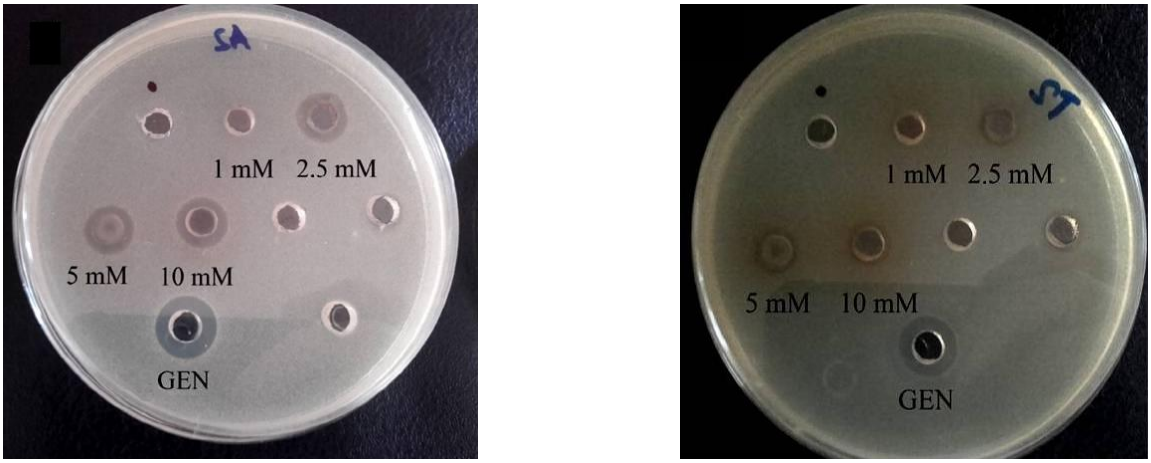

(a) Gram-positive bacteria *S. aureus* after the incubation with the nanoparticles

(b) Gram-negative bacteria *S. typhimurium* after the incubation with the nanoparticles

Fig. 4 Photographs of the Petri dishes containing colonies of bacteria. The concentration of used $AgNO_3$ is provided in the figure. The abbreviation GEN stands for gentamycine

bacteria, with small differences in the effect against particular bacterial strains. Namely, *Bacillus cereus* is definitely more resistant than *Salmonella enterica var. typhimurium*. In all the concentrations (except 1 mM), the nanoparticles caused a growth delay of all tested gram-positive and gram-negative bacteria. It is interesting that increasing the concentration above 2.5 mM generally does not increase the growth delay. The highest inhibition of growth was observed in case of 2.5 mM Ag NPs, although the highest used concentration was four times higher. The results hint to the fact that there is a critical concentration (in our case 2.5 mM), above which further increase does not lead to improved antibacterial activity despite the fact that Ag NPs are more numerous in the case of higher concentrations. The size of Ag NPs definitely also plays a role there.

Our results confirm the observations of the other works utilizing *Origanum vulgare* L. water extract for the synthesis, which also observed a significant antibacterial activity (Sankar *et al*. 2013, Baláž *et al*. 2017b, Shaik *et al*. 2018).

The first question arises from the comparison of our results with those in the pilot study by Sankar *et al*. (2013), as the same concentration (1 mM), the same way of extract preparation and the same OV:Ag ratio (Table 1) was used in both studies. In the present study, we did not observe any antibacterial activity, whereas the authors of the mentioned study did (for some bacterial strains they report inhibition zones larger than 10 mm, for some smaller). However, the authors used 30 μL of the water solution with the concentration 0.3 mg/mL concentration of their Ag NPs/OV dry product. In order to isolate the powder product, which was then used for characterization like XRD or FTIR, they must have centrifuged the prepared nanosuspension (although this is not mentioned in the paper), thus the content of Ag was significantly enriched. Of course, not the whole material was silver, as there is also a contribution form the OV matrix, but it is highly probable that its

contribution into overall weight would be minor, as during centrifugation, mainly silver as heavy element should be maintained in solid. Moreover, if the XRD patterns in the solid-state approach (Baláž *et al*. 2017b) and extract-volume dependent study (Shaik *et al*. 2018) are checked, it can be seen that the amorphous region at low 2 theta values and crystalline species different from Ag, respectively, can be found. On the other hand, in Sankar *et al*. (2013), only silver diffractions could be identified, pointing to quite high purity of the NPs without a significant contribution from the plant matrix. Nevertheless, if we consider that only two thirds (0.2 mg) of overall 0.3 mg of material in 1 mL nanosuspension is silver (from our point of view, its content would be higher), we can calculate that there is 6 μg of Ag present in the 30 μL suspension used for antibacterial tests. This hypothesis assumes completely homogeneous distribution of silver. In our case, we have used 90 mL 1 mM $AgNO_3$ solution, which contains 15 mg of silver. This solution was mixed with 10 mL OV extract. Upon calculation, we find that in 50 µL of nanosuspension used for antibacterial tests, there is only 4.9 μg silver in one well. As the content of silver is most probably much higher in the study (Sankar *et al*. 2013), it might be the key to why antibacterial activity was notobserved in our case. This is supported by the fact that when increasing concentration 2.5-fold (the mass of Ag in the well is 12.1 µg for the 2.5 mM sample), a significant antibacterial activity was observed, as the amount of silver was sufficient. From the bacterial strains used in (Sankar *et al*. 2013), only gram-negative *E. coli* was used in our study.

Much more information about the possible effect of precursor concentration on the antibacterial activity can be gained from the comparison with the work (Shaik *et al*. 2018), although the authors have used different perspective, namely changing the volume of the OV extract introduced into the mixture. As already outlined when describing Table 1, the OV:Ag ratio describing the amount of dry *Origanum vulgare* L. available for the interaction with metallic silver was calculated. In Fig. 5, the dependence of the antibacterial activity on this parameter for our study and the data from ref. (Shaik *et al*. 2018) is provided. Four similar bacterial strains (one gram-negative and three gram-positive) were analyzed in both studies, so the results are presented exactly for these lines.

In general, larger inhibition zones were observed in the work (Shaik *et al*. 2018). This is most probably a consequence of larger Ag NPs content in the wells, as although the authors do not report the volume of nanosuspension applied into each well, the concentration of the used $AgNO_3$ solution is in all cases higher than 10 mM (see Table 1). If we hypothesize that they have used 50 μL as we did in our study, the amount of silver in each well would be the same- 54 μg, which is quite a large amount in comparison with our study (4.9 μg for 1 mM, 12.1 μg for 2.5 mM, 24.3 μg for 5 mM and 48.5 μg for 10 mM). Nevertheless, it has been clearly demonstrated in their work that the amount of OV extract plays a significant role on the antibacterial activity, namely the activity became higher when more extract was used. This can be clearly seen from the top part of Fig. 5, in which only the data reported in

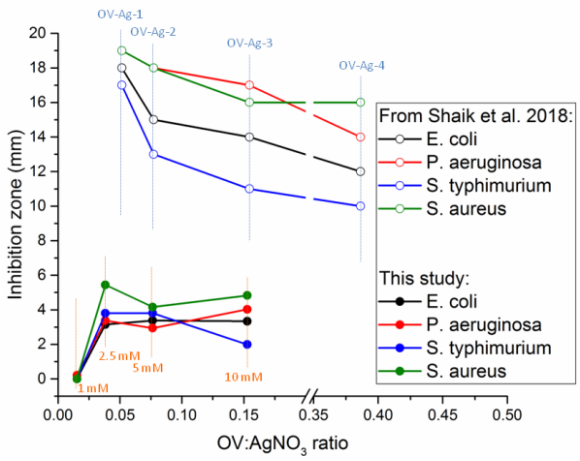

Fig. 5 Dependence of inhibition zone size on the OV: $AgNO_3$ ratio (the results from ref. (Shaik *et al*. 2018) are also used for comparison)

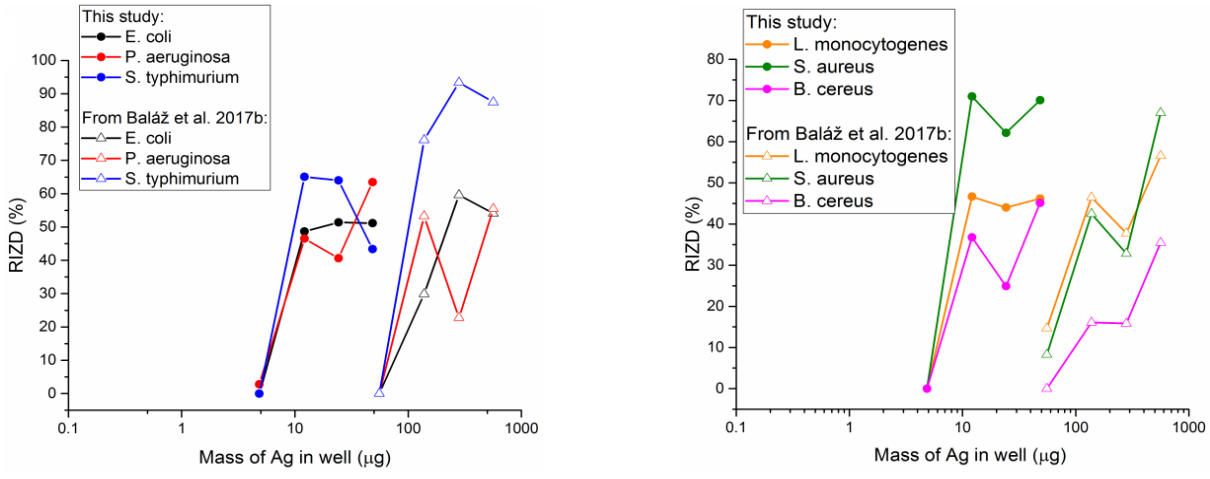

(a) Gram-negative bacteria

(b) Gram-positive bacteria

Fig. 6 Comparison of antibacterial activities observed in ref . (Baláž *et al*. 2017b) and the present study. Modified with permission from ref . (Baláž *et al*. 2017b). Copyright by Elsevier

Shaik *et al*. (2018) are used for comparison with our results. As the authors did not observe activity of the pure OV extract and the content of Ag NPs was the same in all samples, they clearly demonstrated that the antibacterial effect is due to effective distribution in the OV matrix, which becomes better when the amount of plant material is increased. It seems that they did not reach the maximum antibacterial activity (no plateau can be observed), so there is most probably still space to improve the performance.

Our results show different trend, namely the increase of the antibacterial activity when the concentration is increased from 1 mM to 2.5 mM and then more-or-less similar performance. It seems that the maximum antibacterial activity was reached already at 2.5 mM and further increase would be possible only with the increase of the OV extract amount introduced into the system. For both works, the best performance was reached at the $AgNO_3$:OV ratio around 0.05. The general conclusion from comparing the results of recent study with ref. (Shaik *et al*. 2018) is that the antibacterial activity is governed by both amount of Ag NPs and amount of plant extract used. There are definitely ideal conditions, under which the antibacterial activity can be maximized as a result of appropriate selection of both parameters and thus, effective particle size distribution.

The last comparison which can be made is with a solid-state study published in 2017 by our research group (Baláž *et al*. 2017b). The results can be directly compared, as they were performed on exactly the same bacterial strains. The relative inhibition zone diameter is plotted against the amount of silver in one well for all gram-positive and gram-negative bacterial strains and the recent data are compared with those from solid-state approach in Figs. 6(a) and (b), respectively.

Firstly it has to be noted that the calculated mass of Ag in one well in the solid-state approach is not completely correct, as the samples were washed after the synthetic process. During this washing, the residual $AgNO_3$ (which was only minor in the final sample) but also the water-soluble OV substances (which can be very effectively extracted using mechanically activated extraction (Wu *et al*. 2017) and are most probably the major component of the water-soluble fraction) were washed out. So from our point of view, the actual content of Ag would be even higher (similarly as mentioned in the discussion with the study (Sankar *et al*. 2013) earlier). Nevertheless, also the comparison with incorrect lower Ag content from the study (Baláž *et al*. 2017b) is sufficient for comparison, as the content of Ag in well is significantly higher than in the present study even under such circumstances. It is clear that the deposition of silver in the solid-state approach starting from $AgNO_3$:OV weight ratios 1:1 is clearly ineffective, as the antibacterial activity is almost comparable with that of the green-synthetized NPs in the present study working with much lower content of Ag and optimization of the $AgNO_3$:OV ratio would be necessary in future. It has to be stressed out that the x-axis in Fig. 6 is logarithmic, which further emphasizes just mentioned facts. The relative zone of inhibition is almost the same for the same type of bacteria in both works despite the fact that the content of Ag NPs is 10 or more times higher in the solid-state one. Significantly higher activity for the solid-state approach was observed only in the case of *S. typhimurium* strain. The interaction with the active compounds of extract is very important, thus supporting the claims from the study (Shaik *et al*. 2018). The trend of changes in the antibacterial activity with the increased concentration seems to be similar in both studies, however, in the solid-state one, it was the concentration of the produced Ag/ORE composite, whereas in the present one, it is the concentration of the precursor.

4. Conclusions

Silver nanoparticles were successfully synthesized using green approach, concretely the *Origanum vulgare* L. plant water extract. The formation was pursued using five different concentrations of the silver nitrate precursor (1, 2.5, 5, 10 and 100 mM). When the concentration was low, the synthesis was very fast. In the case of 5 mM precursor concentration, it could be well observed by Vis spectra and was finished in 10 minutes. Utilization of higher concentrations resulted in the formation of micro-sized agglomerates, which was also demonstrated by the absence of SPR peak. The PCCS results have shown the finest grain size distribution of the Ag NPs produced by using the $AgNO_3$ precursor with the concentration 2.5 mM. The TEM study of this sample has shown bimodal morphology of produced spherical Ag NPs with larger fraction with size around 100 nm and smaller one with size around 10 nm.

The antibacterial activity was the best for the precursor concentration 2.5 mM and further concentration increase did not result in improvement, thus confirming the most effective size distribution detected for this sample. The in-depth discussion with related works has shown that the antibacterial activity of the OV-mediated Ag NPs synthesis is governed by both extract and $AgNO_3$ concentration. There is some critical amount of Ag NPs necessary for the antibacterial activity to show, but the NPs also need to be effectively distributed within the organic matrix. We are of the opinion that these premises could be valid also for different Ag NPs/plant matrix systems. Finding the proof of this hypothesis could be a motivation for future research.

Acknowledgments

The present study was financially supported by IGA UVLF 13/2016 grant “Antioxidant and antibacterial activity of silver nanoparticles prepared using plant extracts”. The support of the Slovak Research and Development Agency under the contracts No. APVV-14-0103 and that of Slovak Grant Agency VEGA (project 2/0044/18) are also gratefully acknowledged. ND acknowledges financial support from the Slovenian Research Agency (research core funding No. P2-0091).

References

Abbasi, A.M., Shah, M.H., Li, T., Fu, X., Guo, X.B. and Liu, R.H.

(2015), "Ethnomedicinal values, phenolic contents and antioxidant properties of wild culinary vegetables", *J. Ethnopharmacol*., **162**, 333-345.

Abou El-Nour, K.M.M., Eftaiha, A., Al-Warthan, A. and Ammar, R.A.A. (2010), "Synthesis and applications of silver nanoparticles", *Arab. J. Chem*., **3**(3), 135-140.

Agnihotri, S., Mukherji, S. and Mukherji, S. (2014), "Size-controlled silver nanoparticles synthesized over the range 5-100 nm using the same protocol and their antibacterial efficacy", *Rsc Adv*., **4**(8), 3974-3983.

Ahmed, S., Ahmad, M., Swami, B.L. and Ikram, S. (2016), "A review on plants extract mediated synthesis of silver nanoparticles for antimicrobial applications: A green expertise", *J. Adv Res*., **7**(1), 17-28.

Baláž, M., Balážová, Ľ., Daneu, N., Dutková, E., Balážová, M., Bujňáková, Z. and Shpotyuk, Y. (2017a), "Plant-mediated synthesis of silver nanoparticles and their stabilization by wet stirred media milling", *Nanoscale Res. Lett*., **12**, 83-91.

Baláž, M., Daneu, N., Balážová, Ľ., Dutková, E., Tkáčiková, Ľ., Briančin, J., Vargová, M., Balážová, M., Zorkovská, A. and Baláž, P. (2017b), "Bio-mechanochemical synthesis of silver nanoparticles with antibacterial activity", *Adv. Powder Technol*., **28**, 3307-3312.

Beyene, H.D., Werkneh, A.A., Bezabh, H.K. and Ambaye, T.G. (2017), "Synthesis paradigm and applications of silver nanoparticles (AgNPs), a review", *Sustain. Mater. Technol*., **13**, 18-23.

de Souza, T.A.J., Souza, L.R.R. and Franchi, L.P. (2019), "Silver nanoparticles: An integrated view of green synthesis methods, transformation in the environment, and toxicity", *Ecotoxicol. Environ. Safety*, **171**, 691-700.

Deshmukh, S.P., Patil, S.M., Mullani, S.B. and Delekar, S.D. (2019), "Silver nanoparticles as an effective disinfectant: A review", *Mater. Sci. Eng. C-Mater. Biol. Appl*., **97**, 954-965.

Fahimirad, S., Ajalloueian, F. and Ghorbanpour, M. (2019), "Synthesis and therapeutic potential of silver nanomaterials derived from plant extracts", *Ecotoxicol. Environ. Safety*, **168**, 260-278.

Franci, G., Falanga, A., Galdiero, S., Palomba, L., Rai, M., Morelli, G. and Galdiero, M. (2015), "Silver nanoparticles as potential antibacterial agents", *Molecules*, **20**(5), 8856-8874.

Gellé, A. and Moores, A. (2019), "Plasmonic nanoparticles: Photocatalysts with a bright future", *Current Opinion in Green and Sustainable Chemistry*, **15**, 60-66.

Ibrahim, H.M.M. (2015), "Green synthesis and characterization of silver nanoparticles using banana peel extract and their antimicrobial activity against representative microorganisms", *J. Radiat. Res. Appl. Sci*., **8**(3), 265-275.

Iravani, S., Korbekandi, H., Mirmohammadi, S.V. and Zolfaghari, B. (2014), "Synthesis of silver nanoparticles: chemical, physical and biological methods", *Res. Pharmaceut. Sci*, **9**(6), 385-486.

Kang, H., Buchman, J.T., Rodriguez, R.S., Ring, H.L., He, J.Y., Bantz, K.C. and Haynes, C.L. (2019), "Stabilization of Silver and Gold Nanoparticles: Preservation and Improvement of Plasmonic Functionalities", *Chem. Rev*., **119**(1), 664-699.

Khan, M., Khan, S.T., Khan, M., Adil, S.F., Musarrat, J., Al-Khedhairy, A.A., Al-Warthan, A., Siddiqui, M.R.H. and Alkhathlan, H.Z. (2014), "Antibacterial properties of silver nanoparticles synthesized using Pulicaria glutinosa plant extract as a green bioreductant", *Int. J.of Nanomed.*, **9**, 3551-3565.

Kravets, V., Almemar, Z., Jiang, K., Culhane, K., Machado, R., Hagen, G., Kotko, A., Dmytruk, I., Spendier, K. and Pinchuk, A. (2016), "Imaging of Biological Cells Using Luminescent Silver Nanoparticles", *Nanoscale Res. Lett*., **11**, art. ID 30.

Lee, S.W., Chang, S.H., Lai, Y.S., Lin, C.C., Tsai, C.M., Lee, Y.C., Chen, J.C. and Huang, C.L. (2014), "Effect of Temperature on the Growth of Silver Nanoparticles Using Plasmon-Mediated Method under the Irradiation of Green LEDs", *Materials*, **7**(12), 7781-7798.

Liang, C.H., Chan, L.P., Ding, H.Y., So, E.C., Lin, R.J., Wang, H.M., Chen, Y.G. and Chou, T.H. (2012), "Free radical scavenging activity of 4-(3,4-dihydroxybenzoyloxymethyl) phenyl-O-beta-D-glucopyranoside from Origanum vulgare and its protection against oxidative damage", *J. Agricult. Food Chem*., **60**(31), 7690-7696.

Liao, C.Z., Li, Y.C. and Tjong, S.C. (2019), "Bactericidal and Cytotoxic Properties of Silver Nanoparticles", *Int. J. Molecul. Sci*., **20**(2).

Mabey, T., Cristaldi, D.A., Oyston, P., Lymer, K.P., Stulz, E., Wilks, S., Keevil, C.W. and Zhang, X.L. (2019), "Bacteria and nanosilver: the quest for optimal production", *Critical Rev. Biotechnol*., **39**(2), 272-287.

Malik, P. and Mukherjee, T.K. (2018), "Recent advances in gold and silver nanoparticle based therapies for lung and breast cancers", *Int. J. Pharmaceut*., **553**(1-2), 483-509.

Maria, B.S., Devadiga, A., Kodialbail, V.S. and Saidutta, M.B. (2015), "Synthesis of silver nanoparticles using medicinal Zizyphus xylopyrus bark extract", *Appl. Nanosci*., **5**(6), 755-762.

McGillicuddy, E., Murray, I., Kavanagh, S., Morrison, L., Fogarty, A., Cormican, M., Dockery, P., Prendergast, M., Rowan, N. and Morris, D. (2017), "Silver nanoparticles in the environment: Sources, detection and ecotoxicology", *Sci. Total Environ*., **575**, 231-246.

Mogensen, K.B. and Kneipp, K. (2014), "Size-Dependent Shifts of Plasmon Resonance in Silver Nanoparticle Films Using Controlled Dissolution: Monitoring the Onset of Surface Screening Effects", *J. Phys. Chem. C*, **118**(48), 28075-28083.

Ning, S.Y., Wu, Z.X., Dong, H., Yuan, F., Ma, L., Jiao, B. and Hou, X. (2015), "Tunable lasing on silver island films by coupling to the localized surface plasmon", *Optical Mater. Express*, **5**(3), 629-638.

Nookala, S., Tollamadugu, N.V.K.V.P., Thimmavajjula, G.K. and Ernest, D. (2015), "Effect of citrate coated silver nanoparticles on biofilm degradation in drinking water PVC pipelines", *Adv. Nano Res., Int. J*., **3**(2), 97-109.

Pandiarajan, J. and Krishnan, M. (2017), "Properties, synthesis and toxicity of silver nanoparticles", *Environ. Chem. Lett*., **15**(3), 387-397.

Peng, S., McMahon, J.M., Schatz, G.C., Gray, S.K. and Sun, Y.G. (2010), "Reversing the size-dependence of surface plasmon resonances", *Proceedings of the National Academy of Sciences of the United States of America*, **107**(33), 14530-14534.

Rai, M., Yadav, A. and Gade, A. (2009), "Silver nanoparticles as a new generation of antimicrobials", *Biotechnol. Adv*., **27**(1), 76-83.

Rajan, R., Chandran, K., Harper, S.L., Yun, S.I. and Kalaichelvan, P.T. (2015), "Plant extract synthesized silver nanoparticles: An ongoing source of novel biocompatible materials", *Indust. Crops Products*, **70**, 356-373.

Rao, B. and Tang, R.C. (2017), "Green synthesis of silver nanoparticles with antibacterial activities using aqueous Eriobotrya japonica leaf extract", *Adv. Natural Sci.: Nanosci. Nanotechnol*., **8**, art. ID 015014.

Roe, D., Karandikar, B., Bonn-Savage, N., Gibbins, B. and Roullet, J.B. (2008), "Antimicrobial surface functionalization of plastic catheters by silver nanoparticles", *J. Antimicrobial Chemotherapy*, **61**(4), 869-876.

Rojas, J.J., Ochoa, V.J., Ocampo, S.A. and Muñoz, J.F. (2006), "Screening for antimicrobial activity of ten medicinal plants used in Colombian folkloric medicine: A possible alternative in the treatment of non-nosocomial infections", *BMC Complementary Alternat. Med*., **6**, 2.

Roy, K., Sarkar, C.K. and Ghosh, C.K. (2014), "Green Synthesis

of Silver Nanoparticles Using Fruit Extract of Malus Domestica and Study of Its Antimicrobial Activity", *Digest J. Nanomater. Biostruct.*, **9**(3), 1137-1146.

Roy, A., Bulut, O., Some, S., Mandal, A.K. and Yilmaz, M.D. (2019), "Green synthesis of silver nanoparticles: biomolecule-nanoparticle organizations targeting antimicrobial activity", *RSC Adv.*, **9**(5), 2673-2702.

Sankar, R., Karthik, A., Prabu, A., Karthik, S., Shivashangari, K. S. and Ravikumar, V. (2013), "Origanum vulgare mediated biosynthesis of silver nanoparticles for its antibacterial and anticancer activity", *Colloids Surfaces B-Biointerf.*, **108**, 80-84.

Shaik, M.R., Khan, M., Kuniyil, M., Al-Warthan, A., Alkhathlan, H.Z., Siddiqui, M.R.H., Shaik, J.P., Ahamed, A., Mahmood, A., Khan, M. and Adil, S.F. (2018), "Plant-Extract-Assisted Green Synthesis of Silver Nanoparticles Using Origanum vulgare L. Extract and Their Microbicidal Activities", *Sustainability*, **10**(4), art. ID 913.

Sharma, V.K., Yngard, R.A. and Lin, Y. (2009), "Silver nanoparticles: Green synthesis and their antimicrobial activities", *Adv. Colloid Interf. Sci.*, **145**(1-2), 83-96.

Sur, U.K. (2014), "Biological green synthesis of gold and silver nanoparticles", *Adv. Nano Res., Int. J.*, **2**(3), 135-145.

Syafiuddin, A., Salmiati, Salim, M.R., Kueh, A.B.H., Hadibarata, T. and Nur, H. (2017), "A Review of Silver Nanoparticles: Research Trends, Global Consumption, Synthesis, Properties, and Future Challenges", *J. Chinese Chem. Soc.*, **64**(7), 732-756.

Upadhyay, L.S.B. and Verma, N. (2015), "Recent Developments and Applications in Plant-Extract Mediated Synthesis of Silver Nanoparticles", *Anal. Lett.*, **48**(17), 2676-2692.

Velgosova, O., Mrazikova, A. and Marcincakova, R. (2016), "Influence of pH on green synthesis of Ag nanoparticles", *Mater. Lett.*, **180**, 336-339.

Wu, K.J., Ju, T., Deng, Y. and Xi, J. (2017), "Mechanochemical assisted extraction: A novel, efficient, eco-friendly technology", *Trends Food Sci. Technol.*, **66**, 166-175.

CC